Journal of Alloys and Compounds 509 (2011) 8601–8606

Contents lists available at ScienceDirect

Journal of Alloys and Compounds

journal homepage: www.elsevier.com/locate/jallcom

Characterization and corrosion behavior of ceramic coating on magnesium by micro-arc oxidation

Salih Durdu [a], Aylin Aytaç [b], Metin Usta [a,*]

[a] Department of Materials Science and Engineering, Gebze Institute of Technology, Gebze, Kocaeli 41400, Turkey
[b] Gazi University, Faculty of Science, Department of Chemistry, Teknikokullar, Ankara 06500, Turkey

HIGHLIGHTS

- The commercial pure magnesium was coated by micro-arc oxidation method.
- The coating is composed of two layers, a porous outer layer and a dense inner layer.
- A super corrosion resistance was achieved with MAO coatings.
- Coating with Mg_2SiO_4 is more resistant to corrosion than that containing $Mg_3(PO_4)_2$.

ARTICLE INFO

Article history:
Received 6 May 2011
Received in revised form 8 June 2011
Accepted 14 June 2011
Available online 21 June 2011

Keywords:
Micro-arc oxidation (MAO)
Commercial pure magnesium
Corrosion

ABSTRACT

In this study, the commercial pure magnesium was coated in different aqueous solutions of Na_2SiO_3 and Na_3PO_4 by the micro-arc oxidation method (MAO). Coating thickness, phase composition, surface and cross sectional morphology and corrosion resistance of coatings were analyzed by eddy current method, X-ray diffraction (XRD), scanning electron microscope (SEM) and tafel extrapolation method, respectively. The average thickness of the coatings ranged from 52 to 74 μm for sodium silicate solution and from 64 to 88 μm for sodium phosphate solution. The dominant phases on the coatings were detected as spinal Mg_2SiO_4 (Forsterite) and MgO (Periclase) for sodium silicate solution and $Mg_3(PO_4)_2$ (Farringtonite) and MgO (Periclase) for sodium phosphate solution. SEM images reveal that the coating is composed of two layers as of a porous outer layer and a dense inner layer. The corrosion results show the coating consisting Mg_2SiO_4 is more resistant to corrosion than that containing $Mg_3(PO_4)_2$.

1. Introduction

Magnesium and its alloys have high strength to weight ratio, a low elastic modulus, excellent dimension stability, an electromagnetic shielding property, a good damping capacity for reducing noise and vibration, a good manufacturing and machinability. Therefore, they are preferred in the automotive, electronic and aerospace industry fields [1–7]. However, the magnesium and its alloys are extremely susceptible to a galvanic corrosion [8], which can further cause severe pitting corrosion on the metal surface resulting in decreased mechanical stability and unattractive appearance [9]. Its poor corrosion resistance has hindered its widespread use in many applications, especially in acidic environments and in salt-water conditions [10]. In order to overcome corrosion problems, the magnesium can be coated by the micro-arc oxidation method.

The micro-arc oxidation, also called plasma electrolytic oxidation, is one of the new surface modification methods for forming oxide layer on the metal surface [11–17]. Dielectric oxide passive film forms on the metal substrate/electrolyte interface when the sample is applied considerably to a low anodic potential in the electrolyte. In the first stage, discharge channels form in the oxide layer as a result of losing of dielectric stability in the low dielectric region. In this case, micro sparks are observed rapidly to move through the oxide film. Temperatures in the discharge channels vary from 800 to 10,000 K by means of electron collision [18]. Anionic compounds diffuse into the electrolyte due to the presence of electric field. At the same time, the magnesium melted due to the high temperature enters into the discharge channels. So, plasma channels form on the surface. In the second stage, plasma chemical reactions form in the discharge channels. In this case, a pressure increases in the plasma channel and the plasma channels extend to balance the high pressure. Moreover, opposite charged ions are separated due to

* Corresponding author. Tel.: +90 262 6051782; fax: +90 262 6538490.
E-mail address: ustam@gyte.edu.tr (M. Usta).

0925-8388/$ – see front matter © 2011 Elsevier B.V. All rights reserved.
doi:10.1016/j.jallcom.2011.06.059

the existence of electric field. All of cations are pushed out from channels to electrolyte by electrostatic forces. In the last stage, the discharge channels are cooled by electrolyte and reaction products deposit on the channel walls [18–20]. This process that repeats in many different areas causes the coating thickness and surface roughness to increase.

The aim of this study is to increase the corrosion resistance of the commercial pure magnesium coated by the micro-arc oxidation method. The corrosion resistances of micro-arc oxide coatings on the pure magnesium were investigated in varied electrolytic solutions in the literature [21–23]. Mu and Han investigated the corrosion resistances of composite coatings produced in zirconate electrolyte solution [21]. The corrosion resistance in Hanks' solution of composite coatings produced on the pure magnesium was investigated by Shi et al. [22]. The corrosion resistance of coatings produced in $Na_2SiO_3{\cdot}9H_2O$, NaOH and $Na_2B_4O_7{\cdot}10H_2O$ was investigated in SBF (simulated body fluid) by Zhao et al. [23]. The coated samples by MAO have different magnesium oxide phases depending on the parameters such as current density and the electrolyte solution of MAO. Therefore, different phases show a different corrosion behavior. In this study, the different electrolyte solutions of coating from the literature were used to observe the effect of the solution and the current density on the corrosion behavior of the coatings in NaCl solution. Moreover, much corrosive solution than the literature for the corrosion study was used in the current research.

The present work deals with electrochemical investigations of uncoated commercial pure Mg and coated Mg in 3.5 wt.% NaCl aqueous solution. It also investigates the morphological, structural and surface analyses of the coated Mg.

2. Experimental

2.1. Materials and preparation of coatings

Commercial magnesium blocks with the purity of 99.96% were used in this study. Chemical composition of the commercial pure magnesium is given in Table 1. Surfaces of the samples were polished to grits of 400, 800 and 1200 by SiC papers. Then, the samples were cleaned by distilled water and acetone. The electrolyte solutions which consist of 5 g/L $Na_2SiO_3{\cdot}5H_2O$, 1 g/L KOH called as silicate solution and 5 g/L Na_3PO_4, 1 g/L KOH called as phosphate solution were prepared in distilled water. The coatings were produced on the magnesium specimens using micro-arc oxidation (MAO). The MAO coating system that consists of a stainless steel container, cooling and stirring systems was performed with an alternating current (AC) power supply (100 kW). The magnesium substrate and the stainless steel container were used as the anode and the cathode, respectively. Magnesium samples were coated at 0.060, 0.085 and 0.140 A/cm^2 current densities in sodium silicate solutions and sodium phosphate electrolyte solutions for 60 min. After the MAO, the influence of the coating parameters such as the current density and electrolyte concentration on the kinetic, phase composition, microstructure and corrosion resistance of the coatings were investigated.

Coating thicknesses of MAO coatings were measured by using "Fischer Dualscope MP20" device. The characteristics of the coatings were analyzed using an eddy current coating thickness measurement gauge. The phase structures of MAO coatings were analyzed by "Bruker D8 Advance" X-ray diffraction device with scanning between 20° and 80° angles by a scanning speed 2°/min rate.

2.2. Electrochemical measurements

In order to evaluate the anti-corrosion performance of coatings, potentiodynamic polarization and linear polarization studies were carried out using Voltalab 80 Radiometer potentiostat. Specimens used in the electrochemical measurement were mechanically cut into coupons of dimension with 1 cm × 1 cm. The working electrode was inserted in sample holder and its surface area (1.33 cm^2) was in contact with the solution.

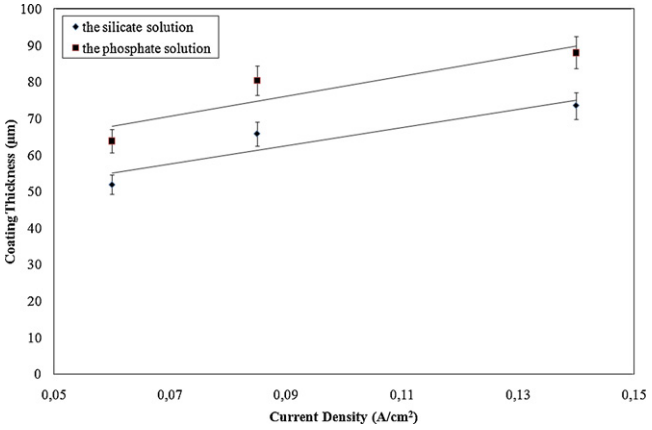

Fig. 1. Variation of coating thicknesses of samples coated at different current densities for 60 min.

Electrochemical experiments were performed in a conventional three electrodes electrochemical cell at 25 °C with a platinum counter electrode and saturated calomel electrode (SCE) with a Lugin capillary. The electrolyte conducting the corrosion tests was the aqueous NaCl solution (Merck) with the concentration of 3.5 wt.%.

Potentiodynamic polarization studies were performed with a scan rate of 1 mV/s in the potential range from −2000 to −1200 mV relative to the corrosion potential. To evaluate the corrosion resistance of coating samples, the Tafel polarization curves of the coatings and Mg substrate were measured in a three-electrode cell. E_{corr}, i_{corr} and corrosion rate obtained from polarization techniques were determined simultaneously by VoltaLab 80 PGZ 301 electrochemical analyzer software.

3. Results and discussion

3.1. Thickness of coatings

Fig. 1 shows that the thickness of the micro-arc oxidized coatings was changed with current density. The average thicknesses of the oxide coatings were measured as 52 μm, 66 μm and 74 μm for 0.060 A/cm^2, 0.085 A/cm^2 and 0.140 A/cm^2 in the silicate solution, whereas they are 64 μm, 80 μm and 88 μm for 0.060 A/cm^2, 0.085 A/cm^2 and 0.140 A/cm^2 in the phosphate solution.

Coatings produced in the phosphate solution were thicker than ones produced in the silicate solution for the same current density. Coatings formed faster in the phosphate solution due to the greater growth rate of coating in the phosphate solution. Although the resistance of the coating electrolyte is increased with decreased current, oxide film grows rapidly on the surface. In addition, the number of micro discharge channels decreases, however, the magnitude of them increases at the high current density. This causes micro discharge channels to provide new electrical paths at a very low resistance. As a result, the coating thickness increased with increasing current as noted in the literature [24].

3.2. Phase structure of coatings

Figs. 2 and 3 illustrate X-ray diffraction results of micro-arc oxide coatings produced in the silicate and phosphate solution, respectively. For coatings produced in the silicate solution, major phases were found to be spinal Mg_2SiO_4 and MgO while the coatings produced in the phosphate solution consists of $Mg_3(PO_4)_2$ and MgO. The existence of MgO phase produced in the both electrolyte solution was observed in the Figs. 2 and 3. The intensity of peaks

Table 1
Chemical composition of the pure magnesium (wt.%).

Al	Ag	Ca	Fe	Mn	Si	Zn	Mg
0.0045	0.0009	0.0004	0.0037	0.0054	0.1480	0.0040	Balance

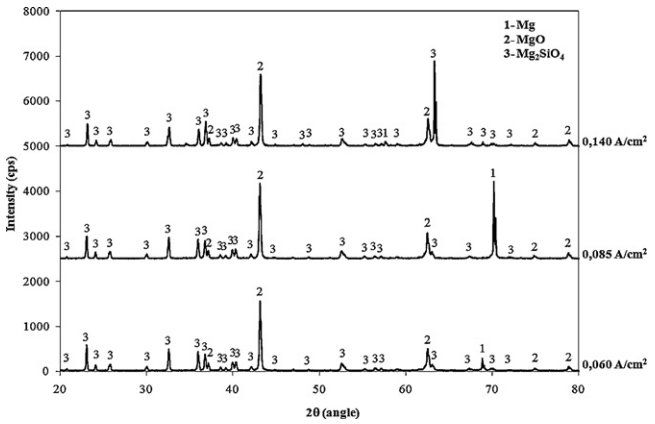

Fig. 2. X-ray diffraction patterns, showing Mg, MgO, Mg_2SiO_4 in the silicate solution.

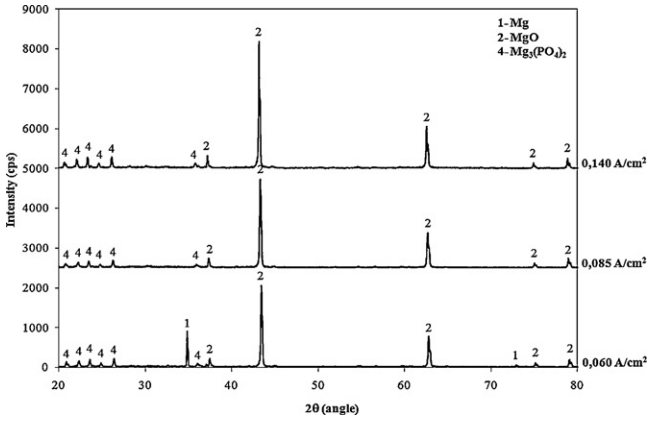

Fig. 3. X-ray diffraction patterns, showing Mg, MgO, $Mg_3(PO_4)_2$ in the phosphate solution.

of MgO produced in the phosphate solution was stronger than the one produced in the silicate solution owing to the thicker coatings produced in the phosphate solution for the same current density. The intensity of XRD peaks of coatings increased due to increasing coating thickness with increasing current density for 60 min in the both electrolyte solution. Si and P anions came from electrolyte solutions. Mg^{2+} cations react with O^{2-} anions and form MgO phase under the high temperature and the high pressure due to the existence of electric field [12]. Mg_2SiO_4 phase forms in the coating structure when MgO and SiO_2 react under the high temperature. Similarly, Mg^{2+} cations which react with $(PO_4)^{3-}$ anions from electrolyte produce $Mg_3(PO_4)_2$.

3.3. Surface and cross sectional morphologies of coatings

Fig. 4 shows the surface morphology of micro-arc oxide coatings. Surface of coatings produced in the phosphate solution has more pores and craters than that of in the silicate solution owing to applying low electric current as a result of losing of dielectric stability. There are many crater-like structures on the coating surface in the early stages of micro-arc oxidation (MAO) process. Also, the surface is considerably porous due to discharge channels on coating surface in the MAO process. In the first stage, the coating has a low surface roughness due to the homogeneous distribution of discharge channels on the surface. When the number of discharge channels decreases with increasing coating thickness resulting in nonuniform coating structure, the surface roughness gradually increases [25]. In addition, the cracks form on the surface due to the thermal stresses [26]. As a result, when the current density increases, the cracks are formed by thermal stresses. Pores on the surface grow with increasing current density and the surface becomes rougher with respect to untreated specimen.

Fig. 5 shows the cross sectional morphologies of coatings produced in both electrolyte solutions at different current densities for 60 min. As shown in SEM images, there is a high density of porosity on the coated surface. Micro-pores on the surface should have a detrimental effect on the corrosion performance, however, only the outer layer consists of porosity and there is almost no porosity in the dense inner layer (Fig. 5). It is reasonable to conclude that the dense inner layer prevented the specimens from the corrosion. As seen in Fig. 5, the dense inner layer increases with increasing the current densities of MAO method. This situation is the same for the silicate and the phosphate solution.

3.4. Polarization measurement

Figs. 6a–c and 7a and b display the typical potentiodynamic polarization and the linear polarization studies of uncoated and coated specimen by micro-arc oxidation in silicate and phosphate electrolyte. The corrosion potentials, corrosion current densities

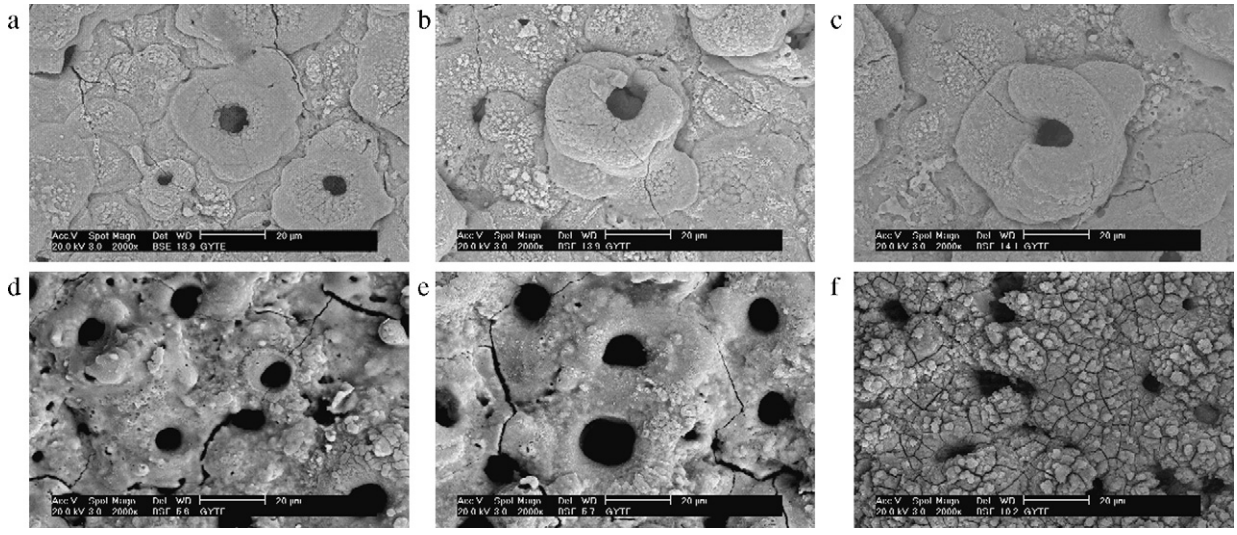

Fig. 4. Surface morphologies of coatings produced in the silicate solution at (a) 0.060 A/cm^2, (b) 0.085 A/cm^2, (c) 0.140 A/cm^2 for 60 min and in the phosphate solution at (d) 0.060 A/cm^2, (e) 0.085 A/cm^2, (f) 0.140 A/cm^2 for 60 min.

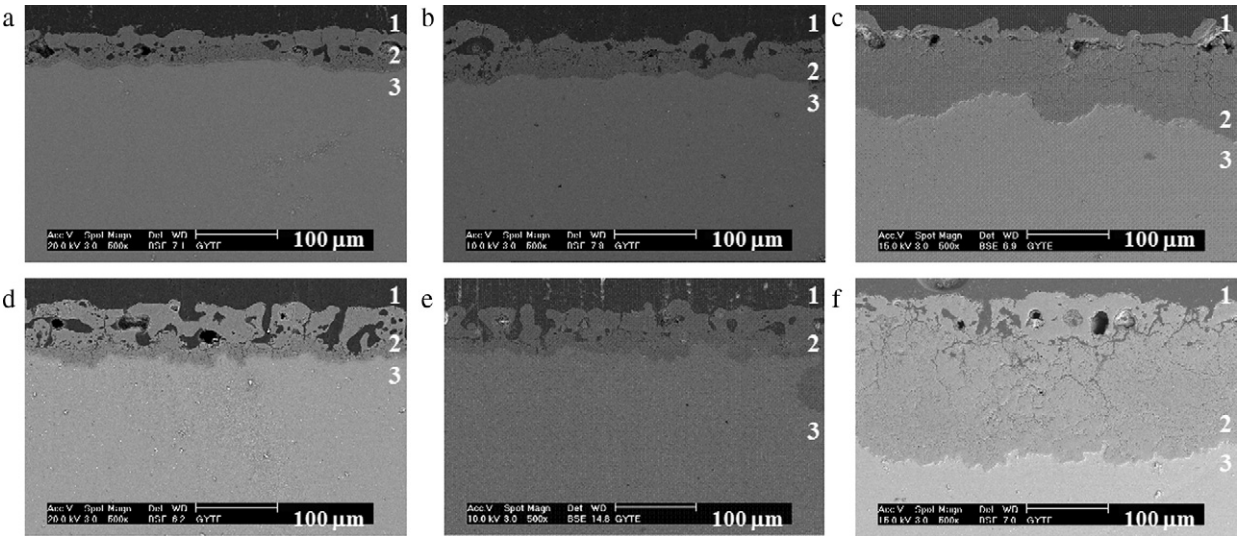

Fig. 5. Cross sectional morphologies of coatings produced in the silicate solution at (a) 0.060 A/cm^2, (b) 0.085 A/cm^2, (c) 0.140 A/cm^2 for 60 min and in the phosphate solution at (d) 0.060 A/cm^2, (e) 0.085 A/cm^2, (f) 0.140 A/cm^2 for 60 min: (1) epoxy resin region, (2) MAO coatings region, (3) the substrate region.

and anodic/cathodic tafel slopes (β_a and β_c) were calculated from these tests. Then, based on the approximate linear polarization at the corrosion potential (E_{corr}), polarization resistance (R_p) values were determined by the Eq. (1) below [27].

$$R_p = \frac{\beta_A \beta_C}{2.3 i_{corr}(\beta_A + \beta_C)} \quad (1)$$

In this equation, i_{corr} refers to the corrosion current density. A summary of the electrochemical corrosion parameters derived from the potentiodynamic polarization curves is listed in Table 2.

The curves of the specimen coated at 0.060, 0.085 and 0.140 A/cm^2 current densities in the silicate solution were shifted from 49 mV, 29 mV and 25 mV to the positive direction and in the phosphate solution they were shifted from 167 mV, 182 mV and 184 mV to the positive direction relative to the curve of the uncoated specimen. This result indicates that the corrosion resistance of the coated specimen is greater than that of the uncoated one.

The corrosion current densities for uncoated specimen decreased from 50.92 μA/cm^2 to 13.65, 2.064 and 4.482 μA/cm^2 at 0.060, 0.085 and 0.140 A/cm^2 in the silicate solution, respec-

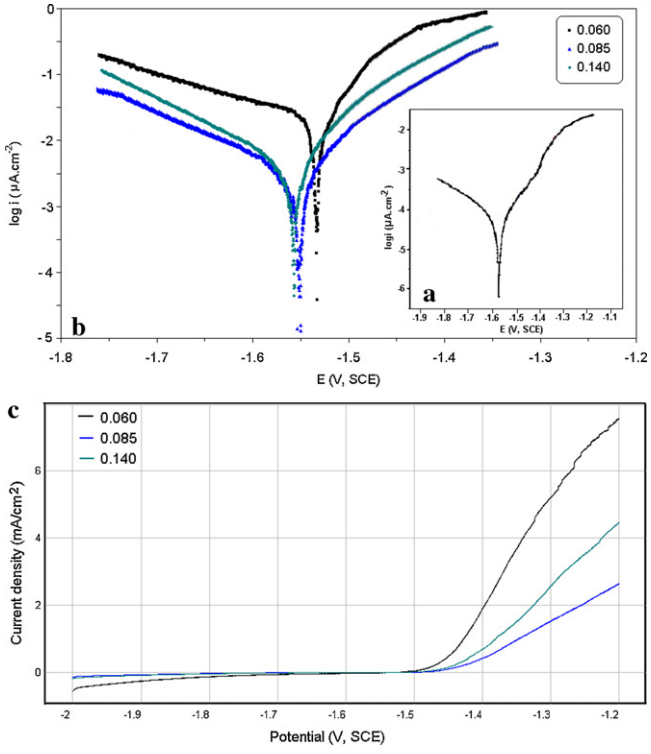

Fig. 6. (a) Potentiodynamic polarization curves of bare Mg and (b) potentiodynamic polarization curves of the coated specimens in the silicate solution at 25 °C, pH 7.3 and open to air after an immersion time of 1 h for stabilization. (c) Linear polarization curves of the coated specimens.

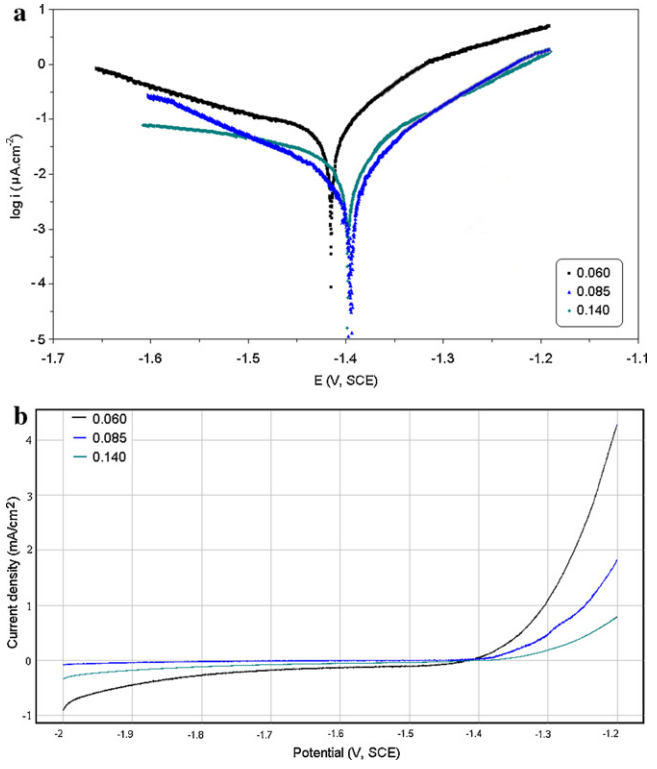

Fig. 7. (a) Potentiodynamic polarization curves of the coated specimens in the phosphate solution at 25 °C, pH 7.3 and open to air after an immersion time of 1 h for stabilization. (b) Linear polarization curves of the coated specimens.

Table 2
Electrochemical parameters related to potentiodynamic polarization curves.

Electrolytes	Electrode	Potentiodynamic polarization			
		Thickness (μm)	$-E_{corr}$ (mV)	i_{corr} (mA/cm^2)	C.R (μm/y)
The silicate solution	Pure Mg	–	1581.5	50.92	1481.0
	0.060	51.9	1532.6	13.65	311.4
	0.085	65.8	1552.9	2.064	47.07
	0.140	73.5	1556.7	4.482	102.2
The phosphate solution	0.060	63.8	1414.9	49.70	1133
	0.085	80.4	1399.5	9.428	215.0
	0.140	88.0	1398.0	13.35	304.4

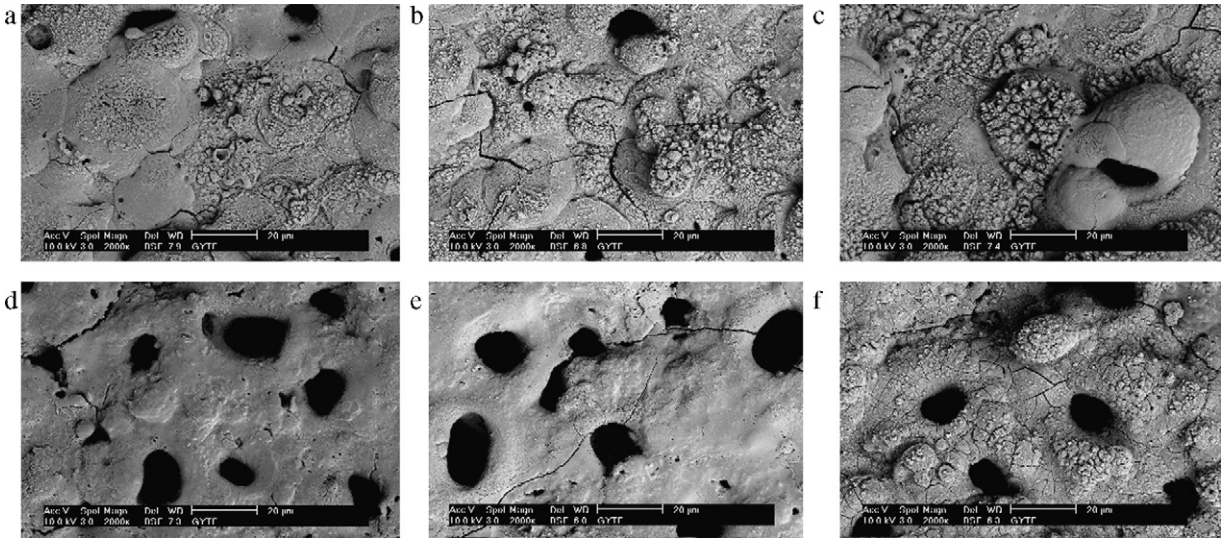

Fig. 8. Surface morphologies of coatings after corrosion test produced in the silicate solution at (a) 0.060 A/cm^2, (b) 0.085 A/cm^2, (c) 0.140 A/cm^2 for 60 min and the phosphate solution at (d) 0.060 A/cm^2, (e) 0.085 A/cm^2, (f) 0.140 A/cm^2 for 60 min.

tively. For the phosphate solution, the corrosion current densities decreased from 64.92 μA/cm^2 to 49.70, 9.428 and 13.35 μA/cm^2, respectively. These values show that the corrosion rates of the coated specimen are lower than 1 mm/y at the silicate solution and 2 mm/y for the phosphate solution. According to the data obtained in this study, it is seen that using the silicate solution resulted higher corrosion resistance for the magnesium in 3.5% NaCl medium. In Fig. 5, some cracks were observed in dense inner layer for the specimen coated at 0.140 A/cm^2 for two different solutions. A little higher corrosion current of the specimen coated at 0.140 A/cm^2 than that of the specimen coated at 0.085 A/cm^2 may be attributable to these cracks. The corrosion resistance of the sample coated in the electrolyte can be attributed to the more uniform and compact structure of this coating which acts as a barrier against the transfer of corrosive ion from aggressive solution into the coating.

Fig. 8 shows the surface morphology of the specimens coated and uncoated with two different solutions after the salt immersion tests for 60 min. Magnesium is an electrochemical active substrate, when a bare specimen is initially immersed in 3.5% NaCl solution. In this condition, hydrogen evolution is seen to occur immediately and the surface is covered with bubbles. The hydrogen bubbles nucleate and periodically are released from the surface. Once pitting initiates, a white precipitate, likely $Mg(OH)_2$ is seen to form around the pits and the alloy surface becomes porous and gray in color [28].

4. Conclusions

Oxide coatings were produced on magnesium using micro-arc oxidation in different aqueous solutions of Na_2SiO_3 and Na_3PO_4. Coatings produced in the phosphate solution were thicker than ones produced in the silicate solution for the same current density. Pores on the surface grow with increasing current density and the surface becomes rougher with respect to untreated specimen. Moreover, the surface of the coatings produced in the phosphate solution has more pores and craters than that of the one produced in the silicate solution owing to applying low electric current as a result of losing of dielectric stability. The corrosion resistance of the sample coated in the electrolyte can be attributed to the more uniform and compact structure of this coating which acts as a barrier against transfer of corrosive ion from aggressive solution into the coating. The corrosion rates of the coated specimen are lower than 1 mm/y at the silicate solution and 2 mm/y for the phosphate solution according to the electrochemical measurements.

Acknowledgements

This work was supported by TUBITAK project (No. 107M476). The authors would like to thank Dr. A. Polat for helping with the preparation of experiment, S. Levent Aktug for running the X-ray diffractometer, A. Nazım for helping with SEM study at Gebze Institute of Technology.

References

[1] J. Guo, L. Wang, J. Liang, Q. Xue, F. Yan, J. Alloys Compd. 481 (2009) 903–909.
[2] J. Liang, B. Guo, J. Tian, H. Liu, J. Zhou, T. Xu, Appl. Surf. Sci. 252 (2005) 345–351.
[3] R. Zhang, D. Shan, E. Han, S. Guo, Trans. Nonferrous Met. Soc. China 16 (2006) 685–688.
[4] V.V. Narulkar, S. Prakash, K. Chandra, Bull. Mater. Sci. 30 (2007) 399–402.
[5] Y. Zhang, C. Yan, Surf. Coat. Technol. 201 (2006) 2381–2386.
[6] J. Liang, L. Hu, J. Hao, Appl. Surf. Sci. 253 (2007) 4490–4496.

[7] X.P. Zhang, Z.P. Zhao, F.M. Wu, Y.L. Wang, J. Wu, J. Mater. Sci. 42 (2007) 8523–8528.
[8] G.L. Song, A. Atrens, Adv. Eng. Mater. 1 (1999) 11–33.
[9] G.L. Song, B. Johannesson, S. Hapugoda, Corros. Sci. 46 (2004) 955–977.
[10] G.L. Song, A. Atrens, Adv. Eng. Mater. 5 (2003) 837–858.
[11] G. Sundararajan, L. Rama Krishna, Surf. Coat. Technol. 167 (2003) 269–277.
[12] H.F. Guo, M.Z. An, H.B. Huo, S. Xu, L.J. Wu, Appl. Surf. Sci. 252 (2006) 7911–7916.
[13] H. Guo, M. An, S. Xu, H. Huo, Thin Solid Films 485 (2005) 53–58.
[14] K. Tillous, T. Toll-Duchanoy, E. Bauer-Grosse, L. Hericher, G. Geandier, Surf. Coat. Technol. 203 (2009) 2969–2973.
[15] J. Liang, L. Hu, J. Hao, Appl. Surf. Sci. 253 (2007) 6939–6945.
[16] J. Ding, J. Liang, L. Hu, Trans. Nonferrous Metal. Soc. China 17 (2007) 244–249.
[17] Z. Shi, G. Song, A. Atrens, Corros. Sci. 48 (2006) 3531–3546.
[18] A.L. Yerokhin, X. Nie, A. Leyland, A. Matthews, S.J. Dowey, Surf. Coat. Technol. 122 (1999) 73–93.
[19] S. Ikonopisov, Electrochim. Acta 22 (1977) 1077–1082.
[20] I. Montero, M. Fernández, J.M. Albella, Electrochim. Acta 32 (1987) 171–174.
[21] W. Mu, Y. Han, Surf. Coat. Technol. 202 (2008) 4278–4284.
[22] P. Shi, W.F. Ng, M.H. Wong, F.T. Cheng, J. Alloys Compd. 469 (2009) 286–292.
[23] L. Zhao, C. Cui, Q. Wang, S. Bu, Corros. Sci. 52 (2010) 2228–2234.
[24] Z. Jiang, X. Zeng, Z. Yao, Rare Metals 25 (2006) 270–273.
[25] L.R. Krishna, K.R.C. Somaraju, G. Sundararajan, Surf. Coat. Technol. 163–164 (2003) 484–490.
[26] F. Chen, H. Zhou, B. Yao, Z. Qin, Q. Zhang, Surf. Coat. Technol. 201 (2007) 4905–4908.
[27] X. Nie, E.I. Meletis, J.C. Jiang, A. Leyland, A.L. Yerokhin, A. Matthews, Surf. Coat. Technol. 149 (2002) 245–251.
[28] T. Lei, C. Ouyang, W. Tang, L.F. Li, L.S. Zhou, Corros. Sci. 52 (2010) 3504–3508.